JOURNAL OF MATERIALS SCIENCE **35** (2000) 271–277

Morphology and fracture behavior in aliphatic polyketones

J. LU, C. K.-Y. LI, G.-X. WEI, H.-J. SUE*
Polymer Technology Center, Department of Mechanical Engineering, Texas A&M University, College Station, TX 77843-3123
E-mail: hjsu@acs.tamu.edu

Morphological features and fracture mechanisms in aliphatic polyketone (PK) samples, prepared via compression molding and injection molding processes, were investigated using differential scanning calorimetry, dynamic mechanical spectroscopy, transmitted optical microscopy and transmission electron microscopy techniques. The PK samples studied are found to have a crystallinity of about 38%. The fracture mechanisms observed in the PK samples are found to be sensitive to strain rate, notch, and stress state. Upon double-notch four-point-bend fracture, the PK fails in a brittle fashion under impact condition and fails in a ductile manner when the testing rate is low. Crazing is the dominant fracture mechanism under the low-rate test conditions, even in the region close to the surface (plane stress region) of the sample. The dominant fracture mechanisms under uniaxial tension are found to be shear yielding and voiding due to debonding of the less-compliant sub-micrometer particles in the PK matrix. No sign of crazing is observed in uniaxial tensile specimens.

1. Introduction

Aliphatic polyketones (PKs) are a new class of semi-crystalline thermoplastics which are obtained by copolymerization of carbon monoxide, ethylene, and/or other olefinic monomers. They have a generalized structure shown below:

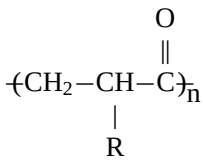

where −R represents either −H or $-CH_3$. When both ethylene and propylene are used as comonomers, their distribution is statistically random [1, 2].

These polymers possess high molecular symmetry and cohesive energy, which lead to excellent thermal, mechanical and barrier properties as well as good chemical resistance [3, 4]. They are attractive for a broad range of engineering applications. Furthermore, in contrast to their aromatic counterparts such as polyetheretherketone (PEEK) and polyetherketone (PEK), which are used for high-performance applications, PKs are produced from simple, inexpensive and abundant monomers, i.e., carbon monoxide, ethylene and/or other olefinic monomers.

A vital consideration for the use of polymers in engineering applications is the need for understanding their fracture behavior. Since PKs are a relatively new class of engineering thermoplastics, knowledge of their fracture behavior is considered critical for their engineering applications.

For decades, the industrial and academic arenas have emphasized research on toughening and strengthening of high performance plastics for structural and automotive applications [5–24]. However, the underlying physics concerning how the toughening mechanisms operate during the fracture process is still not completely understood. Consequently, trial and error is still the prevalent practice for developing tough plastics. A precise methodology for designing tough polymers has yet to be developed.

To avoid the time consuming and sometimes misleading trial and error approach for developing tough polymers and filled plastics, it is imperative that one fully understands the fundamental parameters that govern their fracture behavior. Specifically, the microscopic damage mechanisms and sequence of fracture events have to be known when the polymer fractures. Moreover, damage events should be linked to the material characteristics, such as molecular weight, molecular weight distribution, crystallinity, morphology, etc. To achieve these goals, accurate and effective methods are required to reveal the crack evolution process in these plastics.

The most common approaches in determining the micro-mechanical deformation mechanisms involve inspection of the completely failed specimens using scanning electron microscopy (SEM), optical microscopy (OM), and transmission electron microscopy (TEM)

* Author to whom all correspondence should be addressed.

techniques [6, 20, 22]. Studies of the fracture behavior of plastics relying solely on fracture surface observations using SEM and/or reflected OM usually result in either incomplete understanding or misleading findings concerning exactly how the polymer fails [8, 9, 21, 22, 25]. Investigation of a completely failed specimen, in many cases, may not allow a clear discernment of which factors are responsible for the damage [6, 7, 22]. Tensile dilatometry is sometimes used to delineate the sequence and types of deformation mechanisms [10]. Unfortunately, the low hydrostatic tensile stress component and low testing rate of the tensile tests limit the applicability of these observations to crack-induced failure [9, 21].

The present work focuses on the investigation of morphological features and fracture mechanisms in PK under a variety of testing conditions and sample preparation processes. The double-notch four-point-bend (DN-4PB) technique [26], which is known to be an effective tool for probing the failure mechanisms in toughened polymer systems [8, 9, 21, 23], is used to generate sub-critically propagated cracks. Various microscopy techniques are used to study the damage zone around the sub-critically propagated crack of the DN-4PB specimens.

2. Experimental

2.1. Material and sample preparation

The PK (Carilon® Thermoplastic Polymer DP P1000) used for the present study was provided by Shell Chemical Company. The PK pellets were compression molded into plaques by using a window mold with dimensions of 304.8 × 304.8 × 6.35 mm on a hot press (Dake Hydraulic Press, Model # 935198) under a load of 200 kN at 280 °C. A silicone mold release agent was used to allow clean separation of the PK panel from the mold. Air convection cooling was used to cool the panel to room temperature. The compression molded PK plaques were machined into bars with dimensions of 127 × 12.7 × 6.35 mm. The injection molded tensile bars (ASTM D638 Type I) were investigated "as-received" from Shell Chemical Company.

2.2. Differential scanning calorimetry

The crystalline content of PK samples with different thermal histories, i.e. the "as-received" pellets and the compression/injection molded PKs, was obtained by using a Perkin-Elmer Pyris-1 differential scanning calorimeter (DSC). The melting endotherms were recorded during the temperature scans from 100 to 270 °C at a heating rate of 10 °C/min.

2.3. Dynamic mechanical spectroscopy

PK specimens with dimensions of 42.0 × 12.5 × 3.11 mm were cut from an injection molded tensile bar and dried under vacuum at room temperature for 24 h for dynamic mechanical spectroscopy (DMS) experiments. DMS was performed under torsional mode on a Rheometrics RMS-800 machine. A constant strain amplitude of 0.05% and a fixed frequency of 1 Hz were utilized.

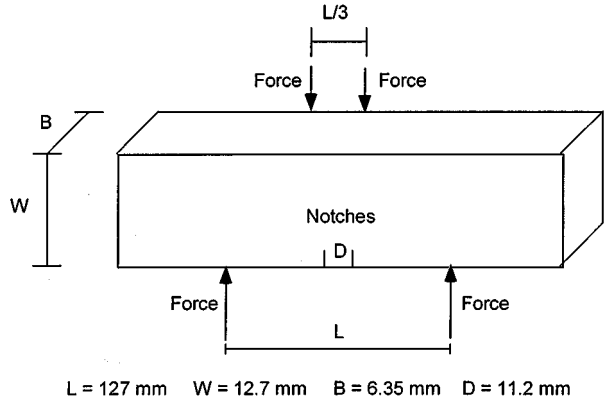

Figure 1 Schematic of the DN-4PB geometry.

The sample was analyzed at temperatures ranging from −140 to 210 °C with 2.5 °C per step.

2.4. Fracture mechanism investigation

The DN-4PB bars were notched with a notching cutter (250 μm tip radius) to a notch depth of 3.18 mm. The distance between the two notches on the DN-4PB bar was set at 11.2 mm to ensure that the two cracks propagate independently from each other (Fig. 1). Sharp cracks were then generated via liquid nitrogen-chilled razor blade tapped at the notch tips. The ratio between the final crack length and the specimen width was held in the range between 0.3 and 0.6.

The DN-4PB tests were performed under both Charpy impact and low loading rate conditions. The Charpy impact test was conducted on a pendulum impact tester (Model TMI-43-02) with a modified double-head striker. For low temperature Charpy impact tests, the specimens and the support were conditioned in an environmental chamber with a temperature setting of −20 °C for at least 20 min. Subsequently, the chamber cover was opened and the test was performed immediately.

A screw-driven mechanical testing machine (Instron, Model 4411) was used to conduct low-rate DN-4PB experiments at ambient temperature. Crosshead speeds of 50.8 and 508 mm/min were used to investigate rate-dependent fracture process in PK.

2.5. Uniaxial tensile test

The uniaxial tensile test was performed using a screw-driven mechanical testing machine (Instron, Model 4411) at ambient temperature. Crosshead speeds of 0.508, 5.08 and 508 mm/min were applied to observe possible ductile and brittle fracture behaviors.

2.6. Microscopy investigations

The DN-4PB damage zone around a sub-critically propagated crack was cut along the crack propagation direction, but perpendicular to the fracture surface, into four sections of approximately equal thickness using a diamond saw (Fig. 2). Both the inner sections (plane strain region) and the surface sections (plane stress region) were polished into thin sections ranging from 50 to 100 μm for transmitted optical microscopy (TOM)

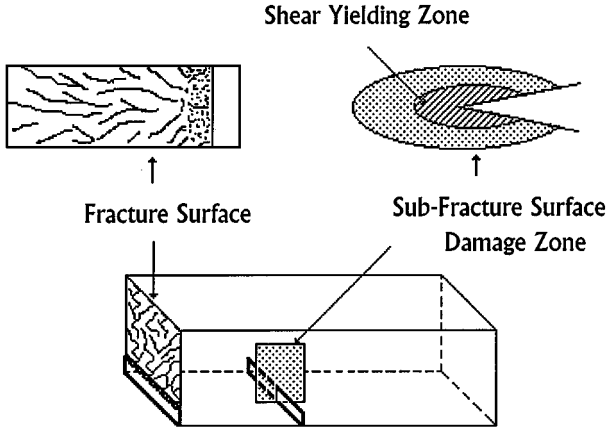

Figure 2 Schematic of the DN-4PB damage zones used for TOM and TEM investigations.

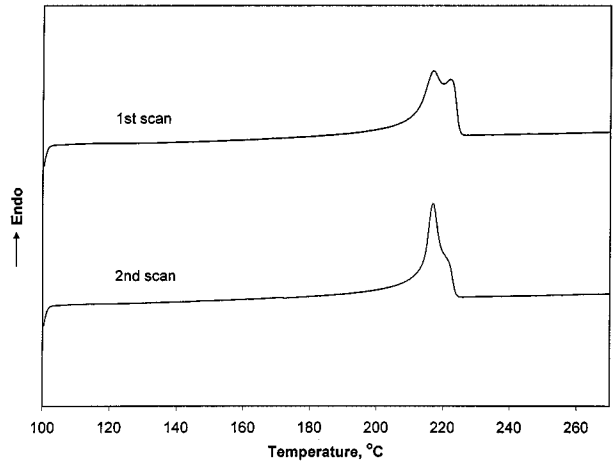

Figure 3 DSC thermograph of the PK pellets.

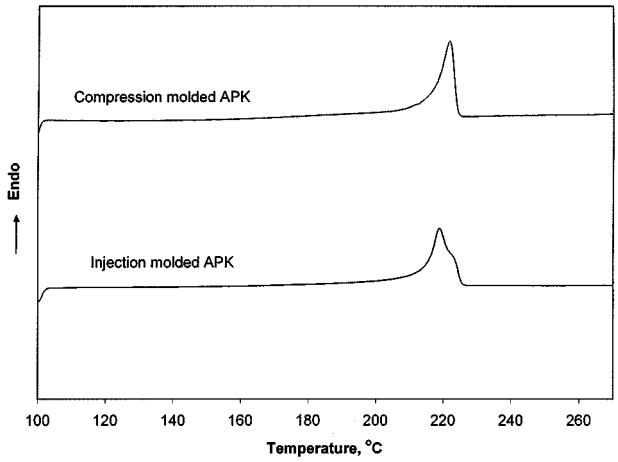

Figure 4 DSC thermographs of compression molded and injection molded PK samples.

investigation. The polishing procedure described by Holik *et al.* was followed [27]. The thin sections were then examined using an Olympus BX60 optical microscope under both bright field and cross-polarization setting. In the TEM experiment, the plane strain region of the damage zone was carefully trimmed to an appropriate size (i.e., an area of about 5×5 mm) and embedded in DER 331 epoxy/diethylenetriamine (12 : 1 ratio by weight). The epoxy was cured at room temperature overnight. The cured block was further trimmed to a size of about 0.3×0.3 mm with the damage zone at the center of the trimmed surface. A glass knife was used to face off the trimmed block prior to RuO_4 staining. The faced-off block was exposed to the vapor of a solution containing 0.2 g of $RuCl_3$ and 10 ml of 5.25% aqueous sodium hypochlorite for 16 h. Ultrathin sections, ranging from 60 to 80 nm thick, were obtained using a Reichert-Jung Ultracut E microtome with a diamond knife. The thin sections were placed on 100-mesh formvar-coated copper grids and examined using a Zeiss-10C TEM operated at an accelerating voltage of 100 kV.

For the uniaxial tensile test specimens, thin sections with dimensions of 10 mm in length and 4 mm in width were carefully cut along the tensile direction from the necked region using a diamond saw. Then, they were polished to 35 μm thick for TOM observations in such a way that the skin region was eliminated and the core region was preserved and analyzed. The sample preparation procedure for TEM observation is the same as described above.

3. Results and discussion

3.1. Differential scanning calorimetry

Fig. 3 shows the DSC thermographs of PK pellets. A bimodal melting peak is observed, i.e., the melting peak is composed of two overlapped peaks. This indicates a bimodal lamellar thickness distribution in the sample [28]. After the first temperature scan was finished, the polymer melt was allowed to cool to 100 °C at 20 °C/min. Then, the second temperature scan was conducted. The melting peak upon the second temperature scan appears to be much different from that of the first temperature scan. A melting peak with a shoulder on the high temperature side is obtained.

The DSC thermographs of the injection molded and compression molded PK samples are shown in Fig. 4. The injection molded PK shows a similar melting peak to that on the second temperature scan of the PK pellets (Fig. 3). A similar bimodal lamellar thickness distribution is also found in polyethylene blown films [29]. It is known that the thickness of crystalline lamellae is primarily determined by crystallization temperature. The higher the temperature at which the crystallization takes place, the thicker the resultant lamellae. The bimodal lamellar thickness distribution in PK pellets is possibly due to the inhomogeneous cooling rate during its solidification process. If the polymer melt is cooled slowly, a relatively homogeneous crystallization temperature can be obtained. The compression molded sample gives an unimodal melting peak and a higher melting point than those of the injection molded sample due to a slower cooling rate of the compression molding process.

The weight percentage crystallinity was calculated by integrating the area under the DSC melting endothermic peak (from 140 to 240 °C), and by comparing the resultant heat of fusion with 100% crystalline PK with the heat of fusion of 227 J/g [4]. The crystallinity of the "as-received" pellets, compression molded and injection molded PKs are found to be 35, 39 and 37%,

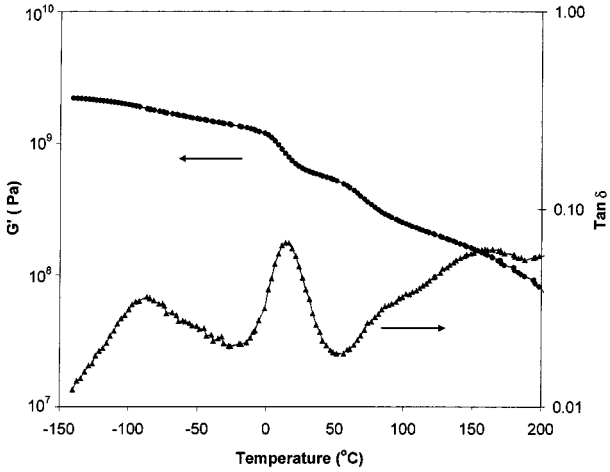

Figure 5 Dynamic mechanical spectrum of injection molded PK sample.

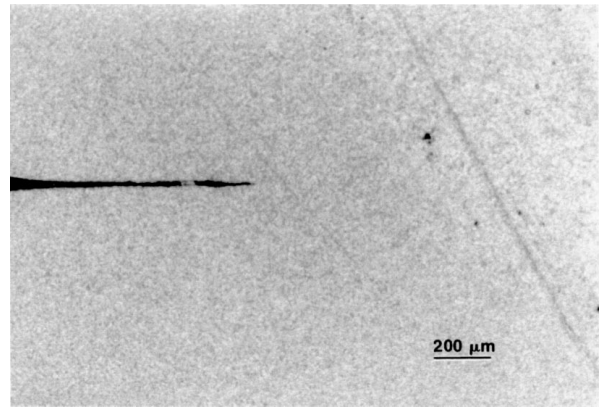

Figure 6 Cross polarization TOM micrograph of the plane strain damage zone of compression molded PK of the DN-4PB-CI (at room temperature) specimen. The crack propagates from left to right.

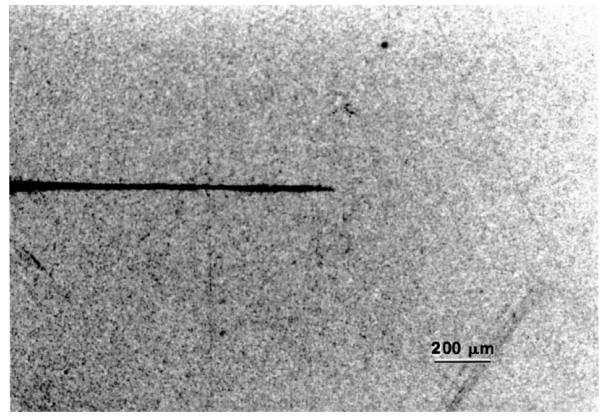

Figure 7 Cross polarization TOM micrograph of the plane strain damage zone of compression molded PK of the DN-4PB-CI (at −20 °C) specimen. The crack propagates from left to right.

respectively. The higher crystallinity of the compression molded PK is due to the slow cooling rate of the compression molding process.

3.2. Dynamic mechanical spectroscopy

The PK studied shows a typical dynamic mechanical spectrum of low crystallinity polymers (Fig. 5). Three distinct relaxation processes, namely α, β, γ relaxations, have been observed for PK below its melting temperature. The α relaxation ranges from about 60 to 190 °C, and obviously can be separated into two subrelaxations known as the α_1 and α_2 relaxations, which may correspond to two different relaxation mechanisms [30]. PK exhibits a highly intensive β relaxation peak centered at around 15 °C. Since the mechanical β relaxation in semicrystalline polymers is somehow equivalent to the glass-rubber transition in amorphous polymers [31], the high intensity of the β relaxation might be attributed to its low crystallinity. The γ relaxation peak of PK is located at about −80 °C. The tan δ vs. temperature curve can usually give information concerning molecular and/or segmental scale motions in polymers. However, unless additional model PK samples are studied here, it is not possible to unambiguously identify the scale and origin(s) of the molecular motion(s) responsible for the formation of both the β relaxation peak and the γ relaxation peak in PK [32].

3.3. Fracture mechanisms

The DN-4PB technique was used to study the fracture mechanisms in PK. Two sets of testing conditions were employed for the PK samples: (i) impact rate (3.5 m/sec) at room temperature (25 °C) and at low temperature (−20 °C), and (ii) low-rate conditions with crosshead speeds of 50.8 and 508 mm/min at room temperature. TOM and TEM were used to investigate the overall fracture process of the DN-4PB damaged samples.

In the DN-4PB Charpy impact (DN-4PB-CI) test at room temperature, the compression molded PK sample shows a featureless crack tip damage zone upon using TOM (Fig. 6). Under crossed-polars, no sign of birefringence is observed. The TOM micrograph of the DN-4PB damage zone obtained at low temperature is very similar to that observed at room temperature (Fig. 7). This indicates a lack of effective toughening mechanism(s) in PK upon DN-4PB-CI fracture at both low temperature and room temperature.

The fracture toughness and operative fracture mechanisms in polymers are affected by both temperature and strain rate. A lower strain rate has the same effect as a higher temperature. It is generally true that the fracture toughness of polymers will increase when the test temperature rises or the strain rate decreases due to viscoelastic behavior of polymers. It is expected that more effective fracture mechanisms, such as shear banding, can be promoted if the test is performed at a slower rate or at a higher temperature.

When the testing rates of 50.8 and 508 mm/min are chosen, significantly larger damage zones are found around the sub-critically propagated cracks in the DN-4PB specimens (Figs 8 and 9). As expected, the damage zone size is larger for the sample tested at 50.8 mm/min. The TOM micrographs of DN-4PB damage zones taken under bright field (not shown) are almost identical to those taken under crossed-polars. No sign of birefringence is found in the damage zones. This

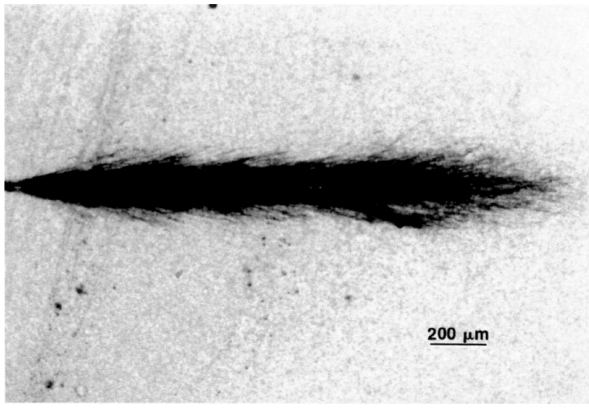

Figure 8 Cross polarization TOM micrograph of the plane strain damage zone of compression molded PK of the DN-4PB (508 mm/min testing rate) specimen. The crack propagates from left to right.

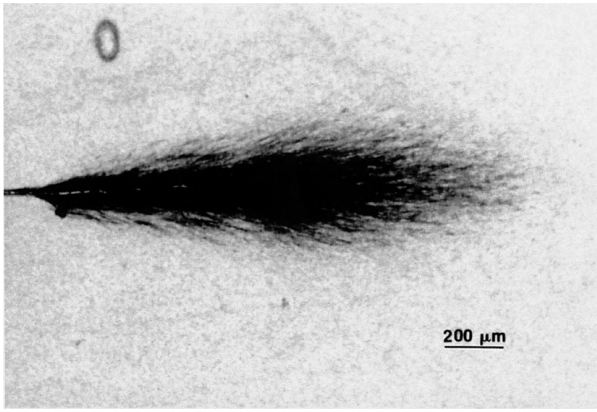

Figure 9 Cross polarization TOM micrograph of the plane strain damage zone of compression molded PK of the DN-4PB (50.8 mm/min testing rate) specimen. The crack propagates from left to right.

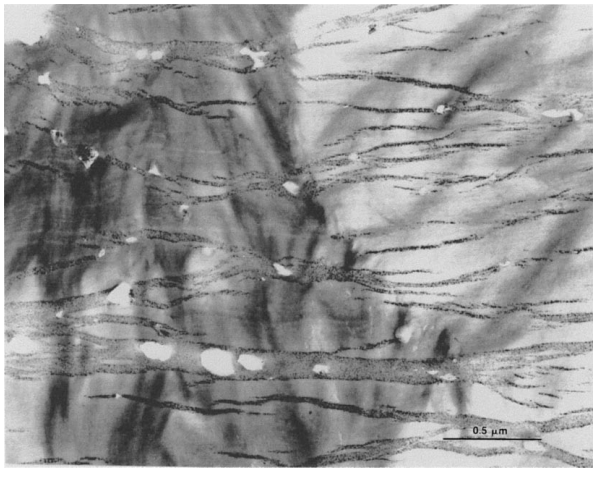

Figure 10 TEM micrograph of compression molded PK sample taken at the DN-4PB (508 mm/min testing rate) damage zone. The crack propagates from left to right.

indicates that no significant shear banding occurs in PK upon DN-4PB fracture.

To study the detailed morphology and fracture mechanisms in PK, TEM investigation was employed. From the TEM micrographs, crazing is the only operative fracture mechanism found in the compression molded

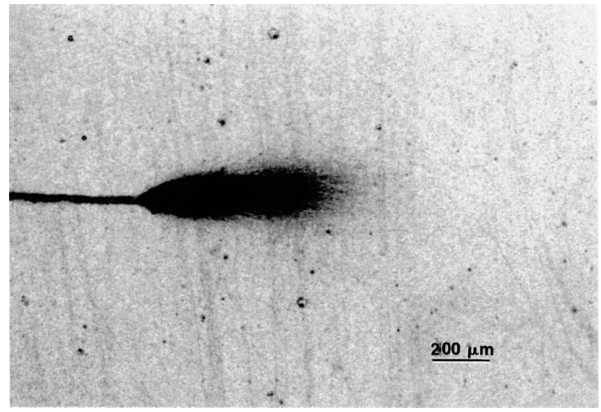

Figure 11 Cross polarization TOM micrograph of the plane stress damage zone of compression modeled PK of the DN-4PB (508 mm/min testing rate) specimen. The crack propagates from left to right. Note that the "thin" crack on the left is the sharp crack generated by the razor blade.

PK sample under low-rate DN-4PB test conditions. Fig. 10 shows the typical crazing pattern in the PK sample. Crazing is a dilatational process favored by triaxial stress state. As expected, the damage zone size in the plane stress region is much smaller when compared with that in the plane strain region (Fig. 11). Nevertheless, Crazing is the primary fracture mechanism both in plane stress and in plane strain regions. No sign of shear banding, which normally occurs in biaxial or uniaxial stress state, could be found, even in the plane stress region. Therefore, it is concluded that the PK sample, upon fracture, behaves more like polystyrene in terms of the propensity to form crazes instead of shear bands. This high tendency to craze may be ascribed to high molecular scale mobility in PK. Most of the craze-prone thermoplastics tend to exhibit a high tan δ peak around room temperature [33, 34].

If shear banding is dominant, fracture usually involves absorption of a significant amount of fracture energy and is considered to be ductile fracture. Crazing is known to precede cracking and is treated as brittle fracture. However, if the craze density is high and is widespread around the crack, then the fracture process may be ductile in nature [35]. Therefore, PK is considered to have failed in a ductile mode under the low testing rates. Only when a sharp crack is present and when the testing condition is impact in nature will PK fail in a brittle manner.

It should be noted that the molecular weight of PK may be another critical parameter affecting the fracture resistance of PK. At this moment, it is still unclear how the molecular weights and crystallinity influence the fracture behavior in PK.

3.4. Uniaxial tensile deformation mechanisms

To further investigate the stress state dependence of the fracture mechanisms in PK, uniaxial tensile tests at various rates of testing were conducted on the "as-received" injection molded tensile specimens. Crosshead speeds of 0.508, 5.08 and 508 mm/min were employed. Surprisingly, even with exhaustive searches under both

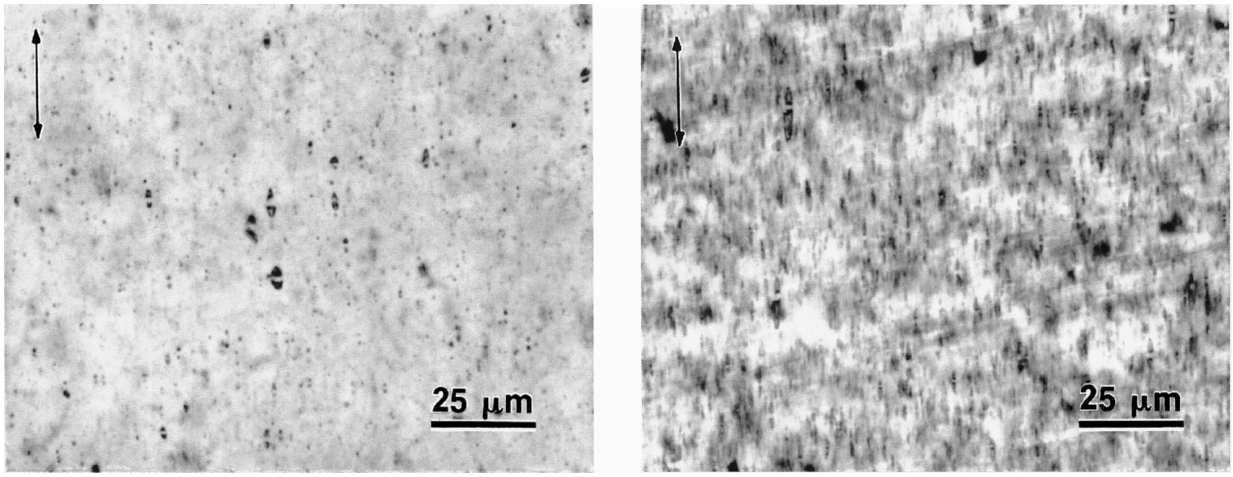

Figure 12 Cross polarization TOM micrograph of PK specimens after uniaxial tensile tests at: (a) 0.508 mm/min testing rate; (b) 508 mm/min testing rate. The arrow indicates the tensile loading direction.

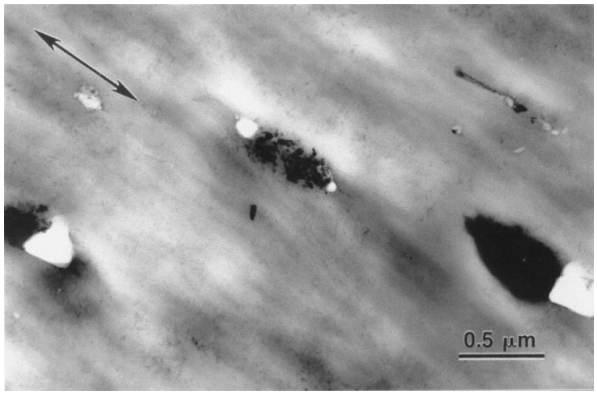

Figure 13 TEM micrograph of PK specimen after uniaxial tensile test at 0.508 mm/min testing rate. The arrow indicates the tensile loading direction.

TOM and TEM, no signs of crazing are found in any of the tensile samples tested. TOM shows that birefringence and voids are present in the necked region of the tensile specimen (Fig. 12). The formation of the voids is probably due to the presence of less compliant and/or poorly adhered sub-micrometer particles (Fig. 13). Therefore, it is concluded that the key deformation mechanism under uniaxial tension is shear yielding.

The brittle-ductile (B-D) transition of polymers can be considered as a competition between a brittle fracture mode and a ductile fracture mode. The B-D transition depends on many testing parameters, such as temperature, strain rate, stress state, pressure, orientation, thickness, and/or notching. PK samples, as expected, can fail in a ductile manner or in a brittle manner. When the crack is blunt, the notched Izod impact strength of PK has been reported to be 220 J/m at room temperature and 50 J/m at $-40\,^{\circ}$C [2]. This impact strength is extraordinarily high among unmodified semicrystalline polymers. However, if a sharp crack is present and the testing rate is high, PK may fail in a brittle manner. This phenomenon is common among all ductile engineering plastics. Even so, it is still unusual to find out that PK is capable of forming such intensive crazes upon fracture.

4. Conclusion

Deformation mechanisms in PK, upon both DN-4PB and uniaxial tensile fractures were investigated. The morphology in PK due to various fabrication processes was also studied. The findings suggest that PK may behave in a ductile manner or in a brittle manner, depending on the test temperature, rate of testing, and the stress state. Crazing is the dominant fracture mechanism for PK upon a low-rate DN-4PB test. PK will fail in a brittle fashion under DN-4PB-CI condition, while it will fail in a ductile manner when the testing rate is low. The DN-4PB damage zone size obtained at low testing rates is much larger than that obtained under the Charpy impact condition. The deformation mechanisms, under uniaxial tensile tests, are found to be primarily shear yielding and voiding due to debonding of the pre-existing particles in the PK matrix. No sign of crazing is found under uniaxial tension.

Acknowledgement

The authors would like to thank Shell Chemical Company for financial support and providing PK samples. Special thanks are given to Drs. J. Kau, P. M. Puccini, and J. W. Kelley for their insightful discussion. Special thanks are also given to Dr. Helga Sittertz-Bhatkar for her experimental assistance on TEM work.

References

1. E. DRENT, U.S. Patent 4.835.250 (1989).
2. R. L. DANFORTH, J. M. MACHADO and J. C. M. JORDAAN, in Proceedings of the 53rd Society of Plastics Engineers Annual Technical Conference (ANTEC), Boston, May 1995, p. 2316.
3. C. E. ASH, D. G. WATERS and A. A. SMAARDIJK, in Proceedings of the 53rd Society of Plastics Engineers Annual Technical Conference (ANTEC), Boston, May 1995, p. 2319.
4. J. E. FLOOD, D. H. WEINKAUF and M. LONDA, in Proceedings of the 53rd Society of Plastics Engineers Annual Technical Conference (ANTEC), Boston, May 1995, p. 2326.
5. A. F. YEE and R. A. PEARSON, *J. Mater. Sci.* **21** (1986) 2462.
6. R. A. PEARSON and A. F. YEE, *ibid.* **21** (1986) 2475.
7. *Idem.*, *ibid.* **24** (1989) 2571.

8. H.-J. SUE, R. A. PEARSON and A. F. YEE, in Proceedings of AICHE 2nd Topical Conference, San Francisco, November 1989.
9. D. S. PARKER, H.-J. SUE, J. HUANG and A. F. YEE, *Polymer* **31** (1990) 2267.
10. C. B. BUCKNALL, "Toughened Plastics" (Appli. Sci. Pub. Ltd., London, 1977) p. 195.
11. W. BASCOM, R. TING, R. J. MOULTON, C. K. RIEW and A. R. SIEBERT, *J. Mater. Sci.* **16** (1981) 2657.
12. J. SULTAN and F. MCGARRY, *Polym. Eng. Sci.* **13** (1973) 19.
13. S. KUNZ-DOUGLASS, P. W. R. BEAUMONT and M. F. ASHBY, *J. Mater. Sci.* **15** (1980) 1109.
14. S. WU, *Polymer* **26** (1985) 1855.
15. A. G. EVANS, Z. B. AHMAD, D. G. GILBERT and P. W. R. BEAUMONT, *Acta Metall.* **34** (1986) 79.
16. A. J. KINLOCH, S. J. SHAW, D. A. TOD and D. L. HUNSTON, *Polymer* **24** (1983) 1341.
17. R. J. M. BORGGREVE, R. J. GAYMANS, J. SCHUIJER and J. F. INGEN HOUSZ, *ibid.* **28** (1987) 489.
18. H. BREUER, F. HAAF and J. STABENOW, *J. Macromol. Sci.-Phys.* **B14**(3) (1977) 387.
19. F. J. GUILD and R. J. YOUNG, *J. Mater. Sci.* **24** (1989) 2454.
20. S. Y. HOBBS and M. E. J. DEKKERS, *ibid.* **24** (1989) 1316.
21. H.-J. SUE and A. F. YEE, *J. Mater. Sci.* **24** (1989) 1447.
22. *Idem., ibid.* 26 (1991) 3449.
23. H.-J. SUE, Ph.D. thesis, The University of Michigan, Ann Arbor, Michigan, 1988.
24. *Idem., Polym. Eng. Sci.* **31** (1991) 275.
25. H.-J. SUE and A. F. YEE, *J. Mater. Sci.* **28** (1993) 2915.
26. H.-J. SUE, R. A. PEARSON, D. S. PARKER, J. HUANG and A. F. YEE, *Polym. Prepr.* **29** (1988) 147.
27. A. S. HOLIK, R. P. KAMBOUR, S. Y. HOBBS and D. G. FINK, *Microstruct. Sci.* **7** (1979) 357.
28. B. WUNDERLICH, "Macromolecular Physics," Vol. 3 (Academic Press, London, 1980), p. 30.
29. J. LU, B. ZHAO and H.-J. SUE, in Proceedings of the 57th Society of Plastics Engineers Annual Technical Conference (ANTEC), New York, May 1999.
30. H. NAKAYASU, H. MARKOVITZ and D. PLAZEK, *Trans. Soc. Rheol.* **5** (1961) 261.
31. I. M. WARD and D. W. HADLEY, "An Introduction to the Mechanical Properties of Solid Polymers" (John Wiley & Sons Ltd., New York, 1993), p. 187.
32. C. XIAO and A. F. YEE, *Macromolecules* **25** (1992) 6800.
33. N. G. MCCRUM, B. E. REED and G. WILLIAMS, "Anelastic and Dielectric Effects in Polymeric Solids" (John Wiley & Sons Ltd., London, 1967).
34. L. E. NIELSEN, "Mechanical Properties of Polymers" (Reinhold, New York, 1962).
35. H.-J. SUE, P. C. YANG, E. I. GARCIA-MEITIN and M. T. BISHOP, *J. Mater. Sci. Letters* **12** (1993) 1463.

Received 15 April
and accepted 16 July 1999